Biologically Plausible Model of Growing Neurites

Gregor A. Kiddie[1,*], Arjen van Ooyen[2], Bruce P. Graham[1]

[1]*Computing Science and Mathematics Department, Stirling University, Stirling, FK9 4LA, Scotland*
[2]*Netherlands Institute for Brain Research, Meibergdreef 33, 1105 AZ Amsterdam, Netherlands*

*Corresponding Author. Tel +44-1786-467-422; fax: +44-1786-464-551; http://www.cs.stir.ac.uk/.
E-Mail: gak@cs.stir.ac.uk (G.A. Kiddie)

Abstract

To better understand how a real neuron works, knowledge of neuronal growth is required. During growth, a neuron changes many of its topological characteristics over time, forming complex dendritic trees and long, branched axons. Many internal and external factors affect the growth of these neurites. We present a model of dendritic growth as determined by the construction of its internal cytoskeleton. Results indicate that changes in particular parameters can lead to different characteristic tree topologies, as seen in real neurons.

Introduction

The brain can be looked upon from many different levels of organization: systems, maps, layers, networks, neurons, synapses, and molecules (Figure 1; Churchland and Sejnowski, 1992). At each level of organization, the questions can be asked, "What does this do?" and "How does this interact?" At very high levels, these questions can be answered by the psychologists, and at very low levels by the chemists and molecular biologists. To answer both together is the task of computational neuroscientists.

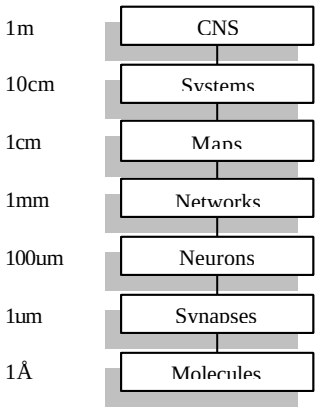

Figure 1. Levels of Organisation.

The model described here spans the levels from molecules to neurons, and has implications for the remaining levels above that. We are interested in how neurons develop, and to this end we present a mathematical model of neurite growth that incorporates known elements of the neurobiology. The aim is to achieve a good working computational model that gives greater insight into neuronal growth processes than simpler, statistical models (van Pelt and Uylings, 1999), and a simulation tool which will accurately run this model and allow it to be easily extended. The basic question to be explored here is what growth mechanisms may contribute to different types of neuron having dendritic trees of different characteristic topology.

Understanding how neurons grow is fundamental to our complete understanding of the formation and operation of real neuronal networks. Insight into the molecular determinants of neuronal growth will be invaluable in developing therapies which require the regrowth of neurons, such as for Alzheimer's disease and repair of spinal cord injuries. Such knowledge will also contribute to neuromorphic technologies for successfully growing neurons on silicon.

Artificial Neural Networks (ANNs) may also benefit from an increased understanding of nervous system development. Typically ANNs use simple network architectures, yet how to design an appropriate network to solve a particular problem is difficult. Even being able to formally specify the number of neurons required is hard. Real neural networks develop in response to a combination of genetic coding and environmental stimuli. Knowledge of what is encoded, and what rules drive network formation in response to real-world signals could lead to design algorithms for ANNs. Our model tackles a small part of this problem in trying to understand the rules underlying the growth of a single neuron's complex dendritic tree. This is a fundamental subproblem for the development of biological neuronal networks.

Theory of Neurite Outgrowth

The theory presented in this paper describes a relatively complex model of interaction between three chemicals identified as proponents of neuronal growth: tubulin, MAP2 and calcium (Figure 2). The interaction between these chemicals results in the production of the rigid cytoskeleton that generates and supports the complex topology of a neuron's dendritic tree.

Tubulin

Tubulin is a molecule that when polymerized forms rigid microtubules which bundle together to give the internal skeleton of a dendrite. Tubulin is produced in the soma and diffuses and is actively transported through the length of the dendrite, until it reaches the terminal, or growth cone. Here, the tubulin molecules are added to the end of the rod-like microtubules, extending their length (Kobayashi and Mundel 1997). This assembly of microtubules results in elongation of the neurite.

The individual microtubules are bundled together to form the rigid cytoskeleton. Branching within the terminal area can be facilitated by the destabilisation of these microtubule bundles, when the bonds tightly binding the microtubules together are relaxed, allowing the microtubules to separate and move in different directions if the conditions are right (Kobayashi and Mundel 1997, Maccioni and Cambiazo 1995).

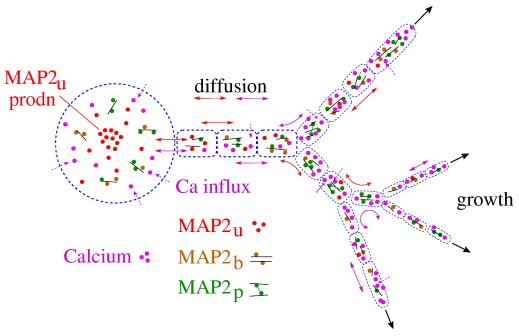

Figure 2. Internals of a growing neurite.

MAP-2

The rates of microtubule assembly and bundling are regulated by microtubule-associated proteins (MAPs). MAP-2 is a specific chemical in this family found in dendrites. The main purpose of MAP-2 in the growing neurite is to bind to the microtubules and stabilise them, thus promoting microtubule assembly and linking them together into bundles (Kobayashi and Mundel 1997, Maccioni and Cambiazo 1995). This stabilising ability depends on the phosphorylation state of the MAP-2 molecules.

Dephosphorylated MAP-2 favours growth as it promotes the assembly and bundling of microtubules. Phosphorylated MAP-2 is more likely to create branching conditions as the microtubule binding is relaxed and they become spaced further apart and are therefore easier to be forced apart by factors such as stress on the growth cone (Audesirk et al, 1997, Friedrich and Aszódi, 1991).

Calcium

Calcium is the mainstay of much of neuronal functioning in both adult and developing neurons. For example, it has major roles in synaptic plasticity and in presynaptic neurotransmitter release. The case of interest here though, is its interaction with the other chemicals involved in neurite outgrowth.

Calcium regulates the rate at which MAP-2 is phosphorylated via a number of biochemical pathways (Hely et al, 2001). Consequently, calcium levels indirectly affect the rate of elongation and branching in a growing neurite. Factors that change the calcium level, such as electrical activity as the result of synaptic input, thus can also influence neurite outgrowth. That is to say, calcium does change the rate of growth and levels of branching, but in a subtle manner, and only as one part of many different elements. It can be looked upon as an effecter of change, rather than the be all and end all of growth.

Other factors

Neurite outgrowth is a highly complex process that involves many factors that are internal and external to the neurite. In addition to the microtubule cytoskeleton, the construction and stability of the actin cytoskeleton in the growth cone at the tip of a growing neurite is also fundamental to the growth process. Filopodia that extend from the growth cone sense the external environment and generate signals in response which influence the state of the internal cytoskeleton.

The aim was to create a biologically plausible model explicitly incorporating only these three chemicals. All other factors are implicit in

model parameters, such as branching and elongation rates. Calcium influx provides a measure of the external environment. We have built upon the original model created by Hely et al. (2001) and have incorporated the numerical techniques for simulating growing neurites developed by Graham and van Ooyen (2001). The model output ultimately will be compared against stochastic models of neurite outgrowth and statistical data from real neurons, as collated by Van Pelt and Uylings (1999).

Methodology

The model of the developing neuron is created in three initial segments: (1) the soma, the cell body in which the tubulin and MAP-2 are produced, (2) an intermediate neurite segment which links the soma to (3) a terminal growth cone segment where the growth is carried out. Each segment is divided into a number of small compartments of length *dx* in which the concentration of the three chemicals is calculated.

The terminal compartment (growth cone) remains of fixed size. Growth is handled by adding new compartments of size *dx* whenever the compartment immediately prior to the growth cone grows to a length of 2**dx* (Figure 3). When this happens, this compartment is split into two compartments, and the process starts again (Graham and Van Ooyen, 2001).

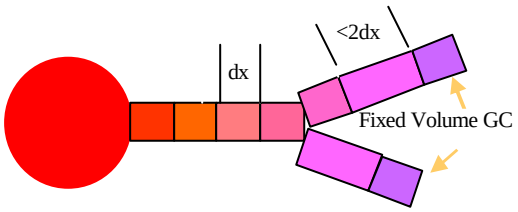

Figure 3. Compartmental Neurite Model.

At each timestep, the terminal compartment has a probability of branching, determined by the concentration of calcium and the phosphorylation state of the MAP-2. A random number is generated, and tested against the branching probability. If the number is higher, elongation is performed as usual, however, if the number is less than the branching probability, two new daughter segments are created in the place of the terminal compartment in such a way that the volume of the compartments is preserved (Hely et al, 2001).

The formulae

The model has been separated up into the three logical parts, the soma, the intermediate compartments, and the terminal compartments. The soma has a simple *production/influx-transport-decay* structure for each chemical. The intermediate compartments have a *transport in – transport out – decay* structure for each chemical. The terminal compartment is more complicated. The calcium retains its influx-diffusion-decay structure. The tubulin has its transport and decay but is now affected by the amount of tubulin that is being assembled and disassembled to and from microtubules. The unbound MAP-2 still has its diffusion and decay but is now affected by the rate at which it is being bound to microtubules. The bound MAP-2 is affected by its decay and its phosphorylation rate, which is a function of calcium. A decay rate and the rate at which it is being converted to and from bound, unphosphorylated MAP-2 determine the amount of phosphorylated MAP-2.

Neurite elongation is a function of the microtubule assembly rate, which depends on the available tubulin and is modulated by bound (unphosphorylated) MAP-2. The terminal branching probability is a function of the relative amount of phosphorylated MAP-2.

Soma

Tubulin

$$\frac{dT_0}{dt} = P + \frac{\hat{D}(T_1 - T_0)}{dx} - hT_0 - d_t T_0$$

= Production – Diffusion –Active Transport - Decay

Unbound MAP-2

$$\frac{dU_0}{dt} = S + \frac{\hat{D}(U_1 - U_0)}{dx} - d_u U_0$$

= Production – Diffusion – Decay

Calcium

$$\frac{dC_0}{dt} = I + \frac{\hat{D}(C_1 - C_0)}{dx} - d_c C_0$$

= Influx – Diffusion – Decay

Intermediate

Tubulin

$$\frac{dT_i}{dt} = \frac{\hat{D}(T_{i+1} - T_i)}{dx} + \frac{\hat{D}(T_{i-1} - T_i)}{dx} + hT_{i-1} - hT_i - d_t T_i$$

= Diffusion In – Diffusion Out +Active Transport In – Active Transport Out - Decay

Unbound MAP-2

$$\frac{dU_i}{dt} = \frac{\hat{D}(U_{i+1} - U_i)}{dx} + \frac{\hat{D}(U_{i-1} - U_i)}{dx} - d_u U_i$$

= Diffusion In – Diffusion Out – Decay

Calcium

$$\frac{dC_i}{dt} = I + \frac{\hat{D}(C_{i-1} - C_i)}{dx} + \frac{\hat{D}(C_{i+1} - C_i)}{dx} - d_c C_i$$

= Influx + Diffusion In – Diffusion Out – Decay

Terminal

Tubulin

$$\frac{dT_t}{dt} = \frac{\hat{D}(T_{t-1} - T_t)}{dx} + hT_{i-1} - d_t T_t - e_t T_t B_t + y_t$$

= Diffusion In +Active Transport In – Decay - Assembly + Disassembly

Calcium

$$\frac{dC_t}{dt} = I + \frac{\hat{D}(C_{t-1} - C_t)}{dx} - d_c C_t$$

= Influx + Diffusion In – Decay

Unbound MAP-2

$$\frac{dU_t}{dt} = \frac{\hat{D}(U_{t-1} - U_t)}{dx} - d_u U_t - c_1 U_t + c_2 B_t$$

= Diffusion In – Decay – Conversion to Bound + Conversion From Bound

Bound (unphosphorylated) MAP-2

$$\frac{dB_t}{dt} = c_1 U_t - c_2 B_t - c_3 F B_t + c_4 G P_t - d_b B_t$$

= Conversion to Bound - Conversion from Bound – Conversion To Phos + Conversion From Phos - Decay

Phosphorylated MAP-2

$$\frac{dP_t}{dt} = c_3 F B_t - c_4 G P_t - d_p P_t$$

= Conversion From Bound – Conversion To Bound - Decay

Elongation

$$\frac{dL}{dt} = e_t T_t B_t - y_t$$

= Assembly – Disassembly

Branching Probability

$$B_{PR} = k_B \frac{P_t}{P_t + B_t}$$

= Probability of branching

Calcium Rate Converters

$$F = \frac{C_t^2}{k_F + C_t^2}$$

= Phosphorylation rate limit

$$G = \frac{C_t^2}{k_G + C_t^2}$$

= Dephosphorylation rate limit

Parameters

There are three sets of parameters used during the simulations: an initial set and two modified sets to generate alternative tree topologies (Tables 1, 2 & 3).

Calcium Influx (I)	0.3
Decay of Calcium (s_c)	0.01
Tubulin Production (P)	0.7
Decay of tubulin (s_t)	0.01
Unbound MAP-2 Production (S)	0.5
Decay of unbound MAP-2 (s_u)	0.3
Active Transport Rate (?)	0.3
Tubulin Assembly Rate (e_t)	0.1
Tubulin disassembly rate ($?_t$)	0.0005
Decay Phosphorylated MAP-2 (s_p)	0.5
Decay of Bound MAP-2 (s_b)	0.3
Conversion Constant 1 (c_1)	0.4
Conversion Constant 2 (c_2)	0.3
Conversion Constant 3 (c_3)	0.4
Conversion Constant 4 (c_4)	0.3
Calcium Rate Constant (F)	0.5
Calcium Rate Constant (G)	0.5
Branching Constant (k_B)	0.01
Diffusion Constant (D)	0.3

Table 1. Initial parameter values.

Conversion Constant 1 (c_1)	0.2
Conversion Constant 2 (c_2)	0.5

Conversion Constant 3 (c_3)	0.5
Conversion Constant 4 (c_4)	0.2
Branching Constant (k_B)	0.01

Table 2. Changes for short terminals.

Conversion Constant 1 (c_1)	0.5
Conversion Constant 2 (c_2)	0.2
Conversion Constant 3 (c_3)	0.2
Conversion Constant 4 (c_4)	0.5
Branching Constant (k_B)	0.01

Table 3. Changes for long terminals

The model is simulated by calculating the concentrations of all chemicals in all compartments at each time step, and performing compartment elongation and branching as necessary. All chemical concentrations start at 0. Simple first-order Euler approximations over time and space are used to discretise the equations. The model is implemented in MATLAB.

Results

The results in figure 4 show that the model can produce several different tree topologies with minimal changes to the parameters. These are consistent with similar topologies produced by Hely's MAP-2 model (Hely et al, 2001) and statistical information from real trees (van Pelt and Uylings, 1999).

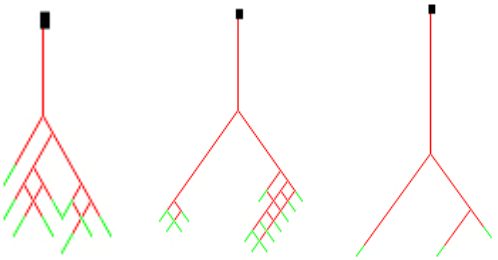

Figure 4. (a) Normal Tree, (b) Short Terminals, (c) Long Terminals.

Figure 5 shows the differences in terminal segment and intermediate segment lengths, with the changes in parameter values. This signifies the ease in which the model can be adapted to produce different neurite topologies. The histograms refer to the type of topology shown in figure 4. Trees of the type shown in figure 4a produce histograms similar to figure 5a. All segments of these trees have the same average length. Trees of type 4b produce histograms similar to figure 5b. These have long intermediate segments and short terminal segments. Trees of type 4c produce histograms similar to figure 5c. These have short intermediate segments and long terminal segments.

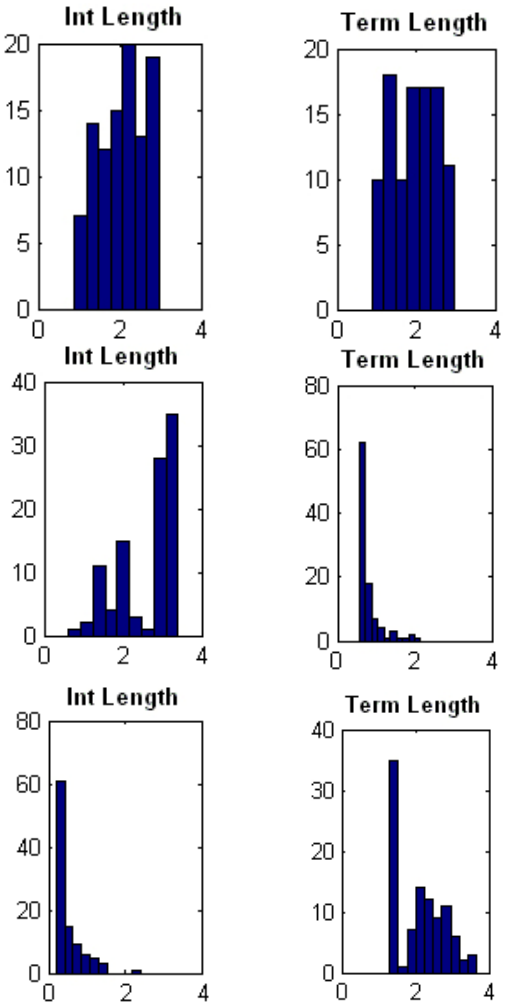

Figure 5. (a) Similar intermediate and terminal lengths (Normal model), (b) Long intermediate and short terminal, (c) Short intermediate and long terminal.

The differences between the three topologies have been generated by the change in rate constants that dictate how much MAP-2 converts to and from its unbound, bound and phosphorylated states.

By increasing the rate that bound MAP-2 is converted into phosphorylated MAP-2 (Constant 3) and reducing the rate that phosphorylated MAP-2 is turned back into Bound MAP-2 (Constant 4), the average amount of phosphorylated MAP-2 increases. This is accentuated by limiting the amount of MAP-2 that becomes bound to microtubules (Constants 1 and 2). This raises the probability of branching and results in longer intermediate segments and shorter terminal segments, as can be seen in figures 4b and 5b.

Decreasing the rate that bound MAP-2 is converted into phosphorylated MAP-2 (Constant 3) and increasing the rate that phosphorylated MAP-2 is turned back into Bound MAP-2 (Constant 4), reduces the amount of phosphorylated MAP-2 and branching decreases. The amount of bound MAP-2 is also raised by an increase in the binding rate from unbound MAP-2 (Constants 1 and 2). This promotes elongation and results in shorter intermediate segments and longer terminal segments, as can be seen in figures 4c and 5c.

Discussion

Model Successes

Real neurons exhibit a wide range of dendritic tree topologies. Particular topologies are characteristic of specific neuronal types. The initial results from our model suggest the differences between the classical neuronal topologies may be due to relatively small differences in the growth process. Here, changes to the rate of binding of MAP-2 to microtubules and the rate of (de)phosphorylation of MAP-2 are sufficient to produce three characteristic classes of tree topology.

These changes in rate constants are an elegant solution to the problem of generating multiple topologies with an essentially similar growth process. Many factors may influence these rate constants in growing neurons, such as the calcium concentration (Hely et al 2001). Calcium levels may change in response to external signalling molecules or due to electrical activity in the neuron. Mechanisms that alter calcium levels and the subsequent effect on neurite outgrowth remain to be fully explored with this model.

The results suggest that the modelled interactions between the three chemicals are close to what they may actually be in reality. If this is the case, then an important and complex area of neuronal growth and the effects upon it have been made more transparent.

Model Limitations

Our model is a very simplified description of neurite outgrowth. Nonetheless, it still contains many different parameters and it remains to further investigate the possibilities of neuronal growth embodied in the model. It will be attempted to accurately match tree topologies with empirically measured statistical data from real neurites (van Pelt and Uylings 1999). This should gain us a greater understanding of the differences in growth between neuronal types.

Currently the parameter values are not necessarily biologically accurate. Some data is available on diffusion and active transport rates, and this will be used to refine the transport parameter values. Some of the parameters are not known. The model results may shed some light upon expected values for parameters such as the rate of change between phosphorylated MAP-2 and bound MAP-2 and how these may be affected by calcium (Hely et al, 2001).

This model can be expanded in several directions. A growth cone with its own cytoskeleton incorporating actin filaments, interacting with an explicit external environment, could be added to allow different means of growth. Growth due to internal pressures, i.e. microtubules pushing the growth cone onward, would combine with external pressures, such as tension on the growth cone due to filopodia sensing attractive cues in different directions, to determine elongation and branching.

Other chemicals which may affect the growth process, and which interact with the chemicals already included in the model could be added. For example, Notch and the Rho family of proteins respond to external signals and are know to affect the stability of the neurite cytoskeleton, altering elongation and branching (Whitford et al, 2002).

Concluding Remarks

There are several interesting inferences that can be taken from the model. Differences between neurons may be genetically encoded in addition to being generated by the situation the neuron finds itself in. The main changes in parameters to produce the different topologies are in the rates of conversion between various states of MAP-2. It can be inferred that the basic rates of change may be one of the “hard coded” elements of the cell’s genetic code. Environmental influences may then further modify these parameters dynamically during growth of a particular neuron.

Control of growth is achieved using only a few factors, allowing the production of a wide variety of topologies with minimal changes to

parameter values. This would likely lead to wide variation in network architecture as well. Understanding how to control neuronal growth is important for new brain therapies that involve regrowing neurons, and new technologies that attempt to interface biological neurons with silicon-based electronics. This indicates how research on underlying mechanisms of real neuronal growth can benefit those in other fields.

Bibliography

[1] Audesirk, G., Cabell, L., Kern, M. 1997. Modulation of neurite branching by protein phosphorylation in cultured rat hippocampal neurons. *Developmental Brain Rresearch*, 102:247-260.

[2] Churchland, P.S., Sejnowski, T.J., 1992, The Computational Brain, *The MIT press.*

[3] Friedrich, P., Aszódi, A. 1991. MAP2: a sensitive cross-linker and adjustable spacer in dendritic architecture. *FEBS*, 295: 5-9.

[4] Graham, B. Van Ooyen, A. 2001. Compartmental models of growing neurites. *Neurocomputing*. 38-40:31-36.

[5] Hely, T. Graham, B. Van Ooyen, A. 2001. A computational model of dendritic elongation and branching based on MAP-2 phosphorylation. *J. Theor. Biol*., 210:375-384

[6] Kobayashi, Naoto. Mundel, Peter. 1997. A role of microtubules during the formation of cell processes in neuronal and non-neuronal cells. *Cell tissue Res*, 291:163-174.

[7] Maccioni, R.B., Cambiazo, V. 1995. Role of Microtubule-Associated Proteins in the Control of Microtubule Assembly. *Physiological Reviews*, 75:835-857.

[8] Van Pelt, J. Graham, B. Uylings, H. 2002. Formation of Dendritic Branching Patterns. In van Ooyen, A., editor, *Modelling Neuronal Development*, chapter 4, pp75-94. MIT Press, Cambridge, MA.

[9] Van Pelt, J. Uylings, H. 1999. Natural Variability in the geometry of Dendritic Branching Patterns. *Modeling in the Neurosciences*. 79-108.

[10] Whitford, K.L., Dijkhuizen, P., Polleux, F., Gosh, A. 2002. Molecular control of cortical dendrite development. *Ann. Rev. Neurosci.* 25:127-149.